PHYSICAL REVIEW B VOLUME 50, NUMBER 24 15 DECEMBER 1994-II

Theory of excitonic exchange splitting and optical Stokes shift in silicon nanocrystallites: Application to porous silicon

E. Martin, C. Delerue, G. Allan, and M. Lannoo
Institut d'Electronique et de Microélectronique du Nord, Département Institut Supérieur d'Electronique du Nord, 41 boulevard Vauban, 59046 Lille Cedex, France
(Received 23 March 1994; revised manuscript received 2 August 1994)

Binding energies and radiative lifetimes of excitons in crystallites are calculated with respect to size and temperature by using a tight-binding configuration-interaction technique. We discuss the recent proposal that, for porous silicon, the exchange splitting could be at the origin of the peculiar behavior of the lifetime and luminescence intensity with temperature, as well as the existence of an onset in selectively excited luminescence. We show that the exchange splitting has no influence on the luminescence lifetime of spherical- or cubic-silicon crystallites because of the spin-orbit and valley-orbit couplings. In contrast, in asymmetrical crystallites, we predict that the spin-orbit and valley-orbit couplings are quenched so that the influence of the exchange splitting can be detected. However, we calculate exchange splittings smaller than the onsets observed in the spectra of the selectively excited luminescence of porous silicon. We show that the Stokes shift induced by the lattice relaxation in the excitonic state is significant and may explain at least partially this decrepancy. We confirm that the direct radiative recombinations are not responsible for the observed decay of the luminescence in porous silicon.

I. INTRODUCTION

Porous silicon is known to emit efficiently light in the visible and infrared range. The infrared emission seems to be connected with the presence of dangling bonds.[1,2] For the visible luminescence, even if its nature is still a source of intense debate, the confinement in silicon crystallites seems to emerge as the main explanation.[3-5] Although porous silicon is a very heterogeneous material on a microscopic scale, some fine structures clearly appear in the excitation spectrum of the visible luminescence at 2 K (Ref. 4) of some porous silicon samples. In particular, an onset of a few meV and, at higher energy, structures associated with phonon-assisted transitions[4,6] are observed. In addition, the lifetime of the visible luminescence decreases going from low (4 K) to higher temperatures ($\sim$100–200 K) in parallel with an increase of the luminescence intensity.[4,7,8] Both effects have been interpreted on the basis of a "two-level model" resulting from the electron-hole exchange splitting,[4,6] which although being smaller than 0.15 meV (Ref. 9) in bulk silicon, could reach a few meV in porous silicon because of the strong confinement.[4,8,10]

Although the two-level model of excitons in nanocrystallites is appealing, it is by nature oversimplified since the exciton states are derived from degenerate valence and conduction bands. The aim of this paper is thus to perform detailed calculations for the excitons, taking into account the manifold of electron and hole states, and their couplings due to Coulomb, exchange, and spin-orbit interactions. In Sec. II we describe the configuration-interaction technique used in the calculation. Section III is devoted to the excitonic band gap of spherical crystallites. The influence of the dielectric constant of the embedding medium is analyzed. In Sec. IV we discuss the excitonic spectra obtained for silicon crystallites with various shapes and conclude that the two-level model can only be justified for very asymmetrical crystallites. We demonstrate that the exchange splitting is indeed enhanced by the confinement but remains smaller than the experimental splittings. In Sec. V we show that this discrepancy can at least be partially explained by the exciton-lattice coupling, which becomes substantial because of the confinement.

II. CALCULATION TECHNIQUE

As the first step, we calculate the one-electron states of the confined silicon crystallites. This is done using a tight-binding framework with the parameters of Ref. 11. Spin-orbit coupling is not yet included in this calculation. The dangling bonds at the surface are saturated by hydrogen atoms to avoid spurious localized states in the band gap. The Hamiltonian matrix is diagonalized using an inverted Lanczos iteration procedure, which allows us to treat large silicon crystallites—up to $\sim$2000 Si atoms—with arbitrary shape. The calculated energies are close to those of our previous calculations,[2] which included the overlaps between atomic orbitals. We have not used the same method here because the treatment of the overlaps in the problem of excitons is computationally tricky and the tight-binding parameters of Ref. 11 give a silicon band structure of reasonable quality. Optical matrix elements are obtained as in Ref. 2, i.e., without the assistance of phonons. This point will be discussed in Sec. IV of the paper.

As the second step, we calculate the excitonic spectrum. We write the exciton wave function as a linear combination of Slater determinants built from the one-electron states. The total Hamiltonian matrix is then expressed in the basis of all these Slater determinants and

 ©1994 The American Physical Society

diagonalized. Actually this is impossible even with the best available computers because the dimension of the basis is too large. It is possible to reduce considerably the number of basis states by only taking into account the Slater determinants corresponding to a single electron-hole excitation. This approximation is justified by the fact that Slater determinants corresponding to n electron-hole excitations ($n \geq 2$) lie at higher energies than single excitations (by $n-1$ times the band-gap energy in the one-electron scheme). If $|\psi_i^c\rangle$ and $|\psi_j^v\rangle$ are, respectively, conduction and valence one-electron states of energy E_i^c and E_j^v, the exciton wave function $|\Psi_{exc}\rangle$ is written as

$$|\Psi_{exc}\rangle = \sum_{i,j} a_{ij} |\psi_j^v \rightarrow \psi_i^c\rangle \ , \qquad (1)$$

where $|\psi_j^v \rightarrow \psi_i^c\rangle$ is the Slater determinant corresponding to the excitation of one electron from the state $|\psi_j^v\rangle$ to the state $|\psi_i^c\rangle$ and a_{ij} are the variational parameters. Then we write the matrix elements of the total Hamiltonian H between the determinants. As shown in Appendixes A and B, the Hamiltonian matrix can be obtained following simple rules:

(i) The diagonal terms contain the one-particle excitation energies $E_i^c - E_f^v$, where E_i^c and E_j^v the one-electron eigenvalues corresponding to $|\psi_i^c\rangle$ and $|\psi_j^v\rangle$.

(ii) The diagonal and nondiagonal terms have two electron repulsion terms $e^2/\epsilon r_{ll'}$ (between electrons 1 and 1′) screened by the appropriate dielectric constant ϵ. Equivalently, they can be expressed as $e^2/\epsilon r_{eh}$ in a two-particle electron-hole formalism.

Finally, the matrix of the total Hamiltonian is diagonalized by standard methods. We also take advantage of the strong confinement in the crystallites. The splittings between the levels can be of the order of several tenths of an eV, which is quite large compared to the other couplings. Therefore, the expansion in Eq. (1) can be limited to a reasonable number of Slater determinants. In practice, we have obtained that the Slater determinants built from the 12 lowest spin states of the conduction band and the 12 highest spin states of the valence band are sufficient. Once the excitonic wave functions are known, we calculate the radiative lifetimes as in Ref. 2.

III. EXCITONIC SPECTRUM OF SILICON CRYSTALLITES

Excitonic band gaps calculated for spherical crystallites are given in Fig. 1. The dielectric constants in the crystallites and in the outside medium are assumed to be the same as in bulk silicon ($\epsilon = 11.7$). The correction to the one-electron band gap is between 0.1 and 0.2 eV, in good agreement with simple effective-mass models.[12] We have verified that the shift in energy from the one-electron band gap is, to a good approximation, given just by the average Coulomb energy between the hole and the electron.[12]

The dielectric constant of the embedding medium is probably very different from the one of crystalline silicon [in porous silicon, it can be, for example, silicon dioxide ($\epsilon \sim 4$) or vacuum ($\epsilon \sim 1$)]. This difference in dielectric

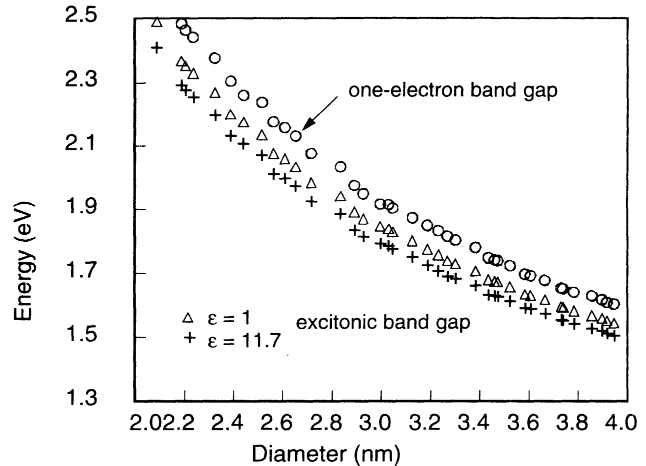

FIG. 1. One-electron band gap (circles) and excitonic band gap calculated for spherical-silicon crystallites with respect to their diameter. For the excitonic band gap, two extreme cases were examined: the outside medium has the same static dielectric constant as bulk silicon (crosses) or the vacuum (triangles).

constant leads to polarization effects (so-called image charge effects), which might become substantial.[13] Polarization terms are given in Ref. 13, for example [Eqs. (3.4) and (4.9), respectively]. Note that the self-polarization and polarization interaction terms are of opposite signs and tend mutually to cancel. With the exciton wave function well approximated by the product of the independent effective-mass wave functions for the electron and the hole, a simple first-order perturbation theory gives for an outside medium with $\epsilon = 1$ a polarization energy shift equal to

$$\Delta E = \frac{0.9077}{R} \ , \qquad (2)$$

where the energy is given in eV and the radius of the crystallite R in angstroms. We see in Fig. 1 that if the shift is substantial, it is much smaller than the confinement energy, which supports our simple perturbation approach. The visible luminescence of porous silicon is in the range of $\sim 1.4-2.2$ eV.[4,14] We see in Fig. 1 that this is compatible with crystallites of diameter between ~ 2.2 and ~ 4.0 nm. Finally, note that the band-gap energy obviously depends on the boundary conditions and could be substantially different with other barriers like silicon oxide.

IV. EXCHANGE SPLITTING IN SILICON CRYSTALLITES

In this section, we discuss the validity of the two-level model[4,8] (Fig. 2). In this model, the lowest exciton level is split into two levels as a result of the exchange interaction between the electron and the hole. The triplet state is the lowest one and the splitting is thought to be in the range of 10 meV because of the confinement. At low temperature ($< \sim 20$ K), only the triplet state is popu-

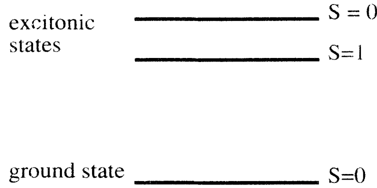

FIG. 2. Two-level model for the recombination of excitons in porous silicon (Refs. 4 and 8). The lowest excitonic state is split due to the exchange interaction between the electron and the hole. The upper level has a much smaller lifetime than the lower one. Thermal equilibrium between the two levels could explain the temperature dependence of the radiative lifetime (Refs. 4 and 8).

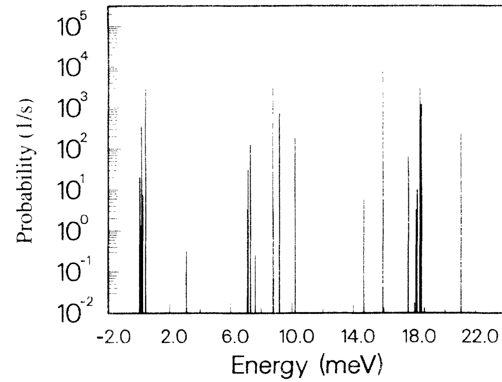

FIG. 3. Calculated excitonic structure of the spherical-silicon crystallite of diameter 3.86 nm. The levels are indicated by vertical bars. The zero of energy corresponds to the lowest exciton level. The height of the bars represents the calculated radiative recombination rate (inverse of the radiative lifetime).

lated and the lifetime is long, in the millisecond range (it is not infinite because the spin-orbit coupling slightly mixes the $S=0$ and $S=1$ states[4]). At higher temperature, the singlet state becomes populated and the radiative recombination is enhanced. The onset energy in selectively excited photoluminescence at 2 K has also been explained by the exchange splitting:[4] At 2 K, the luminescence comes from the triplet state but excitons are predominantly photocreated in the singlet state because the oscillator is inversely proportional to the radiative lifetime.

Wires with varying diameter were suggested as the luminescent structures in porous silicon on the basis of structural analysis. We have thus studied the excitonic spectrum of crystallites with spherical, ellipsoidal, and undulating ellipsoidal shapes. The ellipsoids are defined by $(X/a)^2+(Y/b)^2+(Z/b)^2=1$ where a is larger than b. This can be seen as a deformation of a sphere in one direction X. For the undulating ellipsoids, we introduce an angular fluctuation on the surface of the ellipsoid. This is done using a combination of spherical harmonic functions with arbitrary axes and arbitrary amplitudes. These complex shapes should simulate properly the undulating wires provided that undulations are large enough to localize the excitons.[4]

In Fig. 3, we plot a typical low-energy excitonic spectrum calculated for a spherical crystallite. It is very complicated, with many levels because the electron and hole states are derived from degenerate bands. It was shown in previous works that there are interactions between the conduction states of the different minima and that the induced splittings (valley-orbit splittings) are of the order of 1–10 meV.[2,15] The exciton wave functions built from these one-electron wave functions are also mutually coupled by the Coulomb interaction. Furthermore, we see that the recombination rate of the lowest states (<1 meV in Fig. 3) is not two or three orders of magnitude smaller than those of higher excitonic states so that the radiative lifetime only slightly depends on temperature. This point is verified on all the spherical crystallites even if the excitonic spectrum strongly depends on the crystallite size because of the large variation in the ordering of the valley-orbit split levels.[2] The main explanation of this comes from the spin-orbit coupling. If this one is neglected, some levels have a finite lifetime and the others have an infinite one since the total spin ($S=0$ or $S=1$) is a good quantum number. The spacing of the levels is between 1 and 10 meV, which corresponds to the average valley-orbit splitting and the average exchange integral. When including the spin-orbit coupling, the singlet and triplet states are completely mixed together because this one is of the same amplitude as the spacing between the levels ($\lambda=15$ meV).[11] In consequence, all the levels have on average similar lifetimes and the two-level model is not valid. This would be the same for cubic crystallites or any kind of crystallites in which the x,y,z axes are equivalent by symmetry. This result can be of interest in the perspective of making artificial silicon nanostructures with well-controlled shapes.[16]

For the ellipsoids, the degeneracy of the highest state in the valence band is lifted by the anisotropy. The same is obtained for wires using effective-mass calculations.[17] The highest valence state behaves like p_X for a crystallite in the direction X. If the splitting between the p_X-like state and the other states (p_Y-like and p_Z-like) is large compared to the spin-orbit coupling ($\lambda=15$ meV),[11] then the latter is quenched and the total spin S approximately remains a good quantum number. Because of the strong confinement, already for $a=\sqrt{2}b$ the anisotropy leads to a large splitting (>50 meV) between the p_X-like state and the p_Y- p_Z-like states. However, the excitonic spectrum remains quite complex, with several low-lying states having strongly varying lifetimes because of the remaining degeneracy of the conduction states.

For the undulating ellipsoids, we fix the maximum amplitude of the fluctuation at 25% of the average radius of the ellipsoid. Note that the choice of another amplitude (35%, for example) gives quite similar results. We obtain that all the orbital degeneracies in the valence and conduction bands are lifted. The excitonic spectrum becomes much simpler with the lowest state having systematically a much longer lifetime than the first higher state (see Fig. 4 for a typical example). The two-level

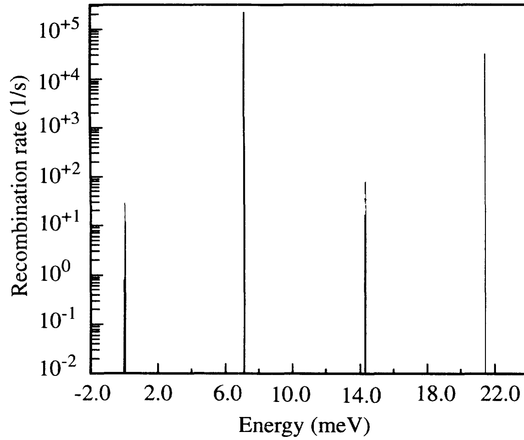

FIG. 4. Calculated excitonic structure of a silicon crystallite with complex shape built from an ellipsoid with a long axis of 2.4 nm, a short axis of 1.8 nm, and 25% of surface undulations. The levels are indicated by vertical bars. The zero of energy corresponds to the lowest exciton level. The height of the bars represents the calculated radiative recombination rate (inverse of the radiative lifetime).

model is then valid to describe such anisotropic crystallites.

In Fig. 5, we plot the calculated splitting Δ between the two lowest excitonic levels for undulating ellipsoids. All the crystallites are characterized by $a=\sqrt{2}b$ and a surface undulation of 25%. The trends in the results do not depend on the ratio between a and b, provided that a is significantly larger than b. The calculation is done for

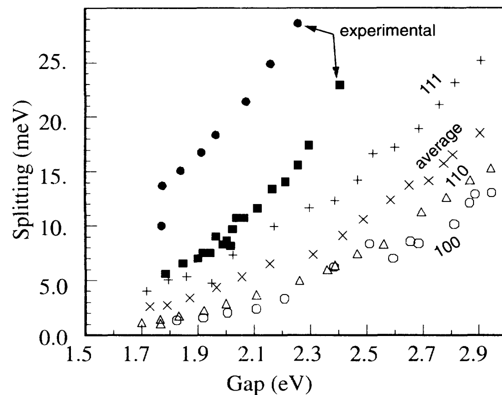

FIG. 5. Splitting between the two lowest calculated excitonic levels in asymmetrical silicon crystallites with respect to their excitonic band gap. Crystallites have undulating ellipsoidal shapes with a longer axis in the 100 direction (open circles), 110 direction (open triangles), and 111 direction (+). Crosses (×) correspond to the average of the splitting over all the orientations of the longer axis of the crystallite. Black squares are the first onsets measured by selectively excited photoluminescence and black dots are the energy splittings derived from the fit of the temperature dependence of the luminescence lifetime of Ref. 4. The black dot at (1.8 eV, 10 meV) is from Ref. 8.

different orientations of the long axis X of the ellipsoid: (100), (110), (111), and an average over all the directions of space. We confirm that the confinement enhances the exchange splitting by two orders of magnitude.[4,8] The (100) direction gives the smallest splitting and the (111) direction the largest one. All other directions of space are intermediate between these two curves. The explanation of this strong dependence on the direction of the main axis of the crystallite is detailed in Appendix B.

In Fig. 5, we compare the calculated splittings with the onset in selectively excited photoluminescence measured in Ref. 4. If the experimental onset corresponds to the smallest exchange splitting among all the crystallites luminescing at the same energy, then we should compare the experimental data with the calculated splittings for the (100)-oriented crystallites. We see that there is a factor 3–5 of discrepancy. The agreement is slightly better for (111)-oriented crystallites but to our knowledge, there is no experimental indication that crystallites are predominantly oriented in (111) directions. The difference with the splittings deduced from the fit of the temperature dependence of the lifetime is still more important. We can note that there is already a large difference between the values at ~ 1.8 eV measured in Refs. 4 and 8.

Before discussing the large discrepancy between theory and experiments, let us compare our calculation with other theoretical work. Published calculations[4,8,10] are based on the effective-mass approximation where the exchange splitting is written as $\Delta = J\int|\varphi(r,r)|^2 d^3r$, where $\varphi(r_e,r_h)$ is the envelope function for the exciton and J is defined as twice the exchange integral per unit inverse volume for the conduction-band-minimum and valence-band-maximum states in bulk silicon.[4] This simple approach is sufficient to show that the exchange interaction increases with the confinement. However, the determination of J is difficult: In Ref. 4, J is indirectly obtained from the exchange splitting of the Ga-2 isoelectronic donor in bulk silicon; in Refs. 8 and 10, it is derived from the experimental knowledge of the higher limit for the exchange splitting of the free exciton in bulk silicon (<0.15 meV).[9] In addition, these experimental values are probably influenced by the effect of the spin-orbit coupling in the same manner as discussed above and, therefore, cannot be easily and directly obtained from experiments.

We now discuss the origin of the discrepancy between our calculated exchange splittings and the observed shifts (Fig. 5). We have seen in Sec. III that the polarization effects have a noticeable influence on the exciton binding energy. But they have a negligible effect on the exchange interaction since the main contributions to the exchange integral come from terms where the electron and the hole are very close (the major contributions are the intra-atomic terms, see Appendix B). In that case, polarization effects must be negligible since the dipole corresponding to the exchange density is extremely small.

A second possible source of problems might come from the variation of the dielectric constant in the crystallite with the confinement. Indeed, as the band gap is opened with increasing confinement, the dielectric constant must decrease. We have calculated the splitting Δ between the

two lowest excitonic levels with respect to the static dielectric constant $\epsilon_{\mathrm{Si}}^{0}$ to see its influence (Fig. 6). Note that when $\epsilon_{\mathrm{Si}}^{0}$ changes, not only Δ but also the excitonic band gap change. A good agreement with experiment could be obtained only for $\epsilon_{\mathrm{Si}}^{0}\sim 3$ if we consider that the onset in selectively excited photoluminescence corresponds to the smallest splitting and not the average. We believe that $\epsilon_{\mathrm{Si}}^{0}=3$ is not a realistic value for the microscopic dielectric constant in silicon crystallites. Recently, Tsu and Babic[18] estimated the effect of the confinement on the dielectric constant. They predict a dielectric constant of ~ 11 for crystallites emitting around 1.5 eV (~ 4 nm) and ~ 6 for crystallites emitting around 2.5 eV (~ 2 nm). The splitting Δ remains in that case quite far from the experimental data. We conclude that, even if the variation of the dielectric constant is not negligible, the onset of the selectively excited photoluminescence cannot be explained by the exchange splitting alone although we have confirmed that its effect may be present in porous silicon.

In Fig. 7, we plot the calculated lifetimes associated with the two lower levels of the undulating ellipsoids. The scattering of the data is important as explained in Ref. 2, which is consistent with the highly nonexponential decay of the luminescence[14] (this nonexponential character can also come from other factors). The difference of two or three orders of magnitude between the lifetimes of the upper and lower levels is in good agreement with experiments.[4] However, our calculated lifetimes are between one and three orders of magnitude larger than the experimental ones, confirming our previous studies.[2] The difference is particularly important for smaller band gaps. Of course, nonradiative recombinations may be important, even if they seem to appear mainly at high temperature (>100 K).[8] Radiative recombination also occurs with the assistance of phonons like in bulk silicon as shown recently by Hybertsen[19] in agreement with experiments.[4] In that case, the influence of the exchange splitting remains because it does not depend on the mechanism of the radiative recombination.

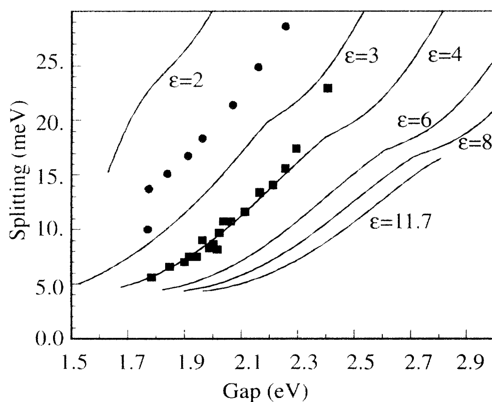

FIG. 6. Splitting between the two lowest excitonic levels with respect to the excitonic band gap calculated for different values of the dielectric constant $\epsilon_{\mathrm{Si}}^{0}$ (lines). The splitting is the average value over all the crystalline orientations. Black squares are the first onsets measured by selectively excited photoluminescence and black dots are the energy splittings derived from the fit to the temperature dependence of the luminescence lifetime of Ref. 4. The black dot at (1.8 eV, 10 meV) is from Ref. 8.

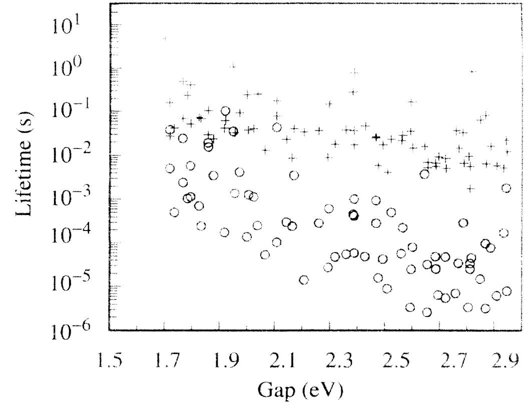

FIG. 7. The calculated lifetimes of the upper (circles) and lower (crosses) excitonic levels with respect to the excitonic energy for the crystallites with complex shapes.

In Ref. 19, substantial differences in the low-temperature decays of the luminescence were reported between the porous silicon samples and those of Ref. 4. (This was also reported for dispersed Si nanocrystallites.[16]) In symmetrical crystallites, we predict that the effect of the exchange splitting vanishes because of the mixing induced by the spin-orbit coupling. It would be interesting to look at the differences in morphology between these samples as suggested in Ref. 19. In the same spirit, anisotropic elastic strains that are present in porous silicon samples[20] can also lift the degeneracies playing the same role as the anisotropy of the confinement.

V. LATTICE RELAXATION IN THE EXCITONIC STATE

In the following, we show that the lattice relaxation in the excitonic state must be substantial. To understand its influence on the selectively excited photoluminescence, let us suppose that the electronic system couples to one-lattice displacement coordinate Q and the equilibrium in the ground state corresponds to $Q=0$. The situation is summarized in the configuration coordinate diagram of Fig. 8, which represents the total energy of a particular crystallite with respect to Q. Since the selectively excited photoluminescence is measured at low temperature (2 K),[4] only the lowest vibronic state is populated in the ground state. Under laser excitation, the maximum of absorption occurs for the vertical transition (arrows (i) in Fig. 8). Then the system relaxes very quickly to its lowest vibronic state, which is centered at $Q=Q_0$. Finally, the radiative recombination appears with a maximum probability at the vertical transition (ii) in Fig. 8. In this simplified view, if the luminescence energy is equal to E_l,

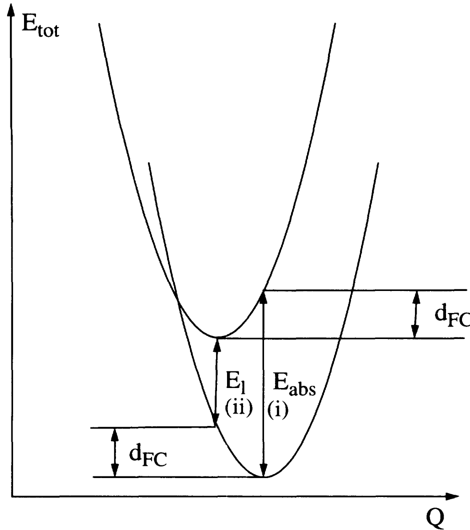

FIG. 8. Configuration coordinate diagram representing the variation of the total energy versus the lattice-displacement coordinate Q. The lowest curve corresponds to the system in its ground state, the upper curve to the excitonic state.

the excitation energy is $E_{abs}=E_l+2d_{FC}$, where d_{FC} is the Franck-Condon shift equal to the energy gain due to lattice relaxation after capture. Therefore, the onset in the selectively excited photoluminescence—the Stokes shift—would be equal to $2d_{FC}$. Of course, the situation is actually more complex, with transitions—in excitation or luminescence—to the different vibronic states of the final states. In the case of a strong lattice coupling, this leads to a Gaussian broadening of the lines centered at the vertical transitions.[21] However, d_{FC} remains the good order of magnitude of the Stokes shift.

The lattice relaxation occurs in the excitonic state because an electron has been transferred from a bondinglike (valence) to an antibondinglike (conduction) state, which tends to weaken the bonds. The local amplitude of the distortion is directly connected to the electron-hole density. The confinement increases this density and, therefore, the Stokes shift is enhanced by the confinement. The variation of the exciton band gap energy with respect to the lattice deformations is described by the deformation potentials. In bulk silicon, by hydrostatic deformations, the deformation potential $a=V(\partial E/\partial V)$ is equal to 1.4 eV for the absolute minimum of the conduction band, to -10 eV for Γ_2', to -0.5 eV for Γ_{15}, and to -5 eV for L_1 minima of the conduction band[22,23] with respect to the top of the valence band ($a=a_c-a_v$). In crystallites where the strong confinement mixes conduction states of the different minima, the deformation potential a must be actually an average of the above values and could vary rapidly with the confinement, with even a change in sign with the confinement. Experimentally, there have been some attempts to measure the pressure dependence of the luminescence or absorption spectra of porous silicon. The measurement is delicate in particular because of the large broadening of the luminescence peak and the

TABLE I. Deformation potentials ($a=dE/d\Delta$) for various porous silicon materials ($a=-BdE/dP$, where dE/dP is the pressure coefficient of the luminescence or optical absorption and B is the bulk modulus).

$a=dE/d\Delta$ (eV)	Ref.
3–5	24
1–3	25
−4 to −9	26
8–10	24
∼7	27

scattering of the results is large as shown in Table I, which collects some values found in the literature.

We have used a simple model based on standard elasticity theory to show that d_{FC} could be substantial in nanostructures. Details are given in Appendix C. The atomic displacements are obtained by minimization of the total energy. The exciton energy depends on the local elastic deformations through the deformation potentials, which are treated as parameters following the previous discussion on their measurement in porous silicon. The Franck-Condon shift d_{FC} is calculated as the difference in energy between the stable configurations of the ground and excited (excitonic) states of the crystallite. Results for d_{FC} are plotted in Fig. 9 for different realistic values of the deformation potentials of the conduction bands Ξ_u and Ξ_d, which enter in the calculation (see Appendix C). We see that the results are sensitive to these values. To get more accurate results, it would be necessary, for example, to make a very careful pseudopotential calculation[23] on crystallites, but this is far beyond the scope of the present paper. In addition, the exciton binding energy can also vary with the relaxation. Anyway, we see that the Franck-Condon shift can be substantial, especially for small crystallites with large band-gap energy.

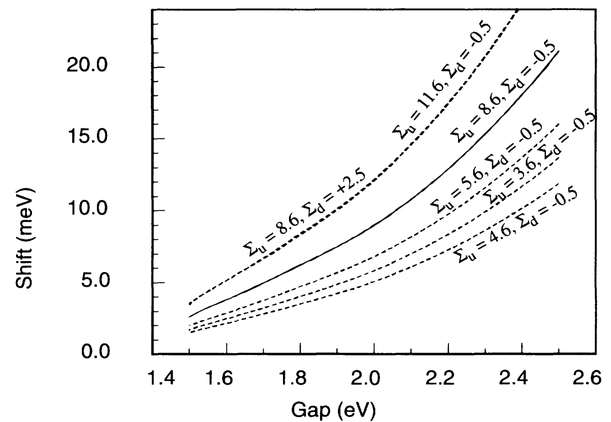

FIG. 9. Calculated Franck-Condon shift with respect to the calculated excitonic band-gap energy. The different curves correspond to different values of the deformation potentials Ξ_d or Ξ_u in eV (the continuous line for the bulk silicon deformation potentials).

Comparing with Fig. 5, we see that the Franck-Condon shift could explain at least partially the difference between the onset observed in the selectively excited photoluminescence and the calculated exchange splitting. More generally, we believe that this work shows that the exciton-lattice coupling in nanocrystallites is important. The coupling is with radial modes, which are mainly derived from low-energy acoustic modes. Therefore, it is probable that multiphonon replica could not be seen in optical spectra but only a broadening.

VI. CONCLUSION

We have calculated the excitonic spectrum of silicon crystallites using an expansion of the exciton wave function in the basis of Slater determinants made from the one-electron confined states. We have shown that the exchange interaction between the electron and the hole does not influence the radiative lifetime of symmetrical crystallitelike spheres. This is mainly due to the spin-orbit coupling. In contrast, in crystallites with asymmetric shapes or subject to anisotropic elastic strains, the exchange splitting must be of visible influence and the system can be reasonably interpreted by a two-level model. However, even in that case, we calculate an exchange splitting much smaller than the onset observed in selectively excited photoluminescence. This discrepancy can be understood at least partially if the Stokes shift induced by the lattice relaxation in the excitonic state is taken into account. We show that this Stokes shift could be as large as the exchange splitting.

ACKNOWLEDGMENT

Institut d'Electronique et de Microélectronique du Nord is UMR No. 9929 of CNRS.

APPENDIX A: DETAILS ON THE EXCITONIC CALCULATION

Here we give details on the computation of the matrix elements of the exciton Hamiltonian. These are obtained assuming that the one-electron states $|\psi_i^c\rangle$ and $|\psi_j^v\rangle$ are solutions of the Hartree-Fock equation where all the valence states $|\psi_j^v\rangle$ are filled by electrons and all the conduction states $|\psi_i^c\rangle$ are empty (notations are defined in Sec. II)

$$\left[\frac{p^2}{2m}-\sum_k \frac{Z_k e^2}{r_k}\right]\psi+\left[\sum_n \int \frac{e^2|\psi_n^v(r')|^2}{|r-r'|}d^3r'\right] - \left[\sum_n \left[\int \frac{e^2\psi_n^{v*}(r')\psi(r')}{|r-r'|}d^3r'\right]\psi_n^v\right]=E\psi\ , \quad \text{(A1)}$$

where ψ can be the states $|\psi_i^c\rangle$ or $|\psi_j^v\rangle$ of energy $E=E_i^c$ or $E=E_j^v$, respectively. We also fix the zero of the total energy for the configuration corresponding to all the electrons in the valence states $|\psi_j^v\rangle$. This method is close to the one developed by Knox in the case of bulk excitons.[28] Following this, we use the screened Hartree-Fock theory and all the Coulomb interactions e^2/r are divided by the dielectric constant $\epsilon_{\rm Si}$ of the electron crystallite. After some algebra, we obtain terms containing the one-electron energies E_i^c and E_j^v, one-particle matrix elements of the spin-orbit coupling $\langle \psi_i|\lambda \boldsymbol{l}\cdot \mathbf{s}|\psi_j\rangle$, and two-particle matrix elements $\langle \psi_i(1)\psi_j(2)(e^2/\epsilon_{\rm Si}r_{12})|\psi_k(1)\psi_l(2)\rangle$ where $\psi_i,\psi_j,\psi_k,\psi_l$ are one-electron wave functions of the valence or the conduction band (including spin). The spin-orbit constant λ is taken from Ref. 11. After development of the one-electron wave functions $\psi_i,\psi_j,\psi_k,\psi_l$ in the atomic-orbital basis, we obtain terms like

$$\left\langle \varphi_{ii}\varphi_{jj}\left|\frac{e^2}{\epsilon_{\rm Si}r_{12}}\right|\varphi_{kk'}\varphi_{ll'}\right\rangle=\int \varphi_{ii}^*(1)\varphi_{jj}^*(2)\frac{e^2}{\epsilon_{\rm Si}r_{12}} \times \varphi_{kk'}(1)\varphi_{ll'}(2)d^3r_1d^3r_2\ . \quad \text{(A2)}$$

In this equation, $\varphi_{ii'}$ is an atomic orbital where the first index i represents the atom and the second one i' the type of the orbital (s,p_x,p_y,p_z). To calculate the integrals of Eq. (A2), some simplifications can be made. If $\varphi_{ii'}$ and $\varphi_{kk'}$ (or $\varphi_{jj'}$ and $\varphi_{ll'}$) do not belong to the same atom $(i\neq k$ or $j\neq l)$, the integral is small and is fixed to zero. This is consistent with the neglect of the overlaps between atomic orbitals in the tight-binding approximation. In the opposite case $(i=k$ and $j=l)$, two situations must be considered. First, when the atoms $i\ (=k)$ and $j\ (=l)$ are distinct, we have terms like $\int \varphi_{ii}^*(1)\varphi_{jj}^*(2)(e^2/\epsilon_{\rm Si}r_{12})\varphi_{ik'}(1)\varphi_{jl'}(2)d^3r_1d^3r_2$. If the wave functions $\varphi_{ii'}$ and $\varphi_{ik'}$ (or $\varphi_{jj'}$ and $\varphi_{jl'}$) are different, the integral is neglected because orbitals are orthogonal. If they are similar, the integral $\int \varphi_{ii'}^*(1)\varphi_{jj'}^*(2)(e^2/\epsilon_{\rm Si}r_{12})\varphi_{ii'}(1)\varphi_{jj'}(2)d^3r_1d^3r_2$ is approximated by $e^2/\epsilon_{\rm Si}^0R_{jj}$ where R_{ij} is the interatomic distance between atoms i and j and $\epsilon_{\rm Si}^0$ is the static dielectric constant. This is justified by the fact that the atomic orbitals are localized on the atoms. Second, when $i=j=k=l$, we have Coulomb and exchange integrals between atomic orbitals of the same atom. They are calculated from atomic wave functions and with the q-dependent dielectric constant of Ref. 30. Details are given in Appendix B.

APPENDIX B: INTRA-ATOMIC COULOMB AND EXCHANGE INTERACTIONS

Here we briefly describe the evaluation of the intra-atomic exchange and Coulomb integrals. We have three types of Coulomb integrals U_{ss}, U_{sp}, U_{pp} where, for example,

$$U_{ss}=\int \frac{|\varphi_s(1)|^2|\varphi_s(2)|^2}{\epsilon_{\rm Si}r_{12}}dr_l^3\,dr_2^3\ , \quad \text{(B1)}$$

where φ_s is the $3s$ atomic orbital of silicon. The main difficulty of the calculation is the dielectric constant $\epsilon_{\rm Si}$ of the silicon crystallite. $\epsilon_{\rm Si}$ is normally dependent on the position of the particles 1 and 2 in Eq. (B1) to take into account the shape of the crystallite. However, the form of the dielectric constant is not known. For simplicity, we assume that $\epsilon_{\rm Si}$ has the same position dependence as in bulk silicon. Using the Fourier transform of Eq. (B1),

we obtain

$$U_{ss}=16\pi^2\int_0^\infty [\rho(q)]^2\frac{1}{\epsilon_{\mathrm{Si}}(q)}dq \; , \tag{B2}$$

where

$$\rho(q)=\frac{2}{\sqrt{2}\pi q}\int_0^\infty r|\varphi_s(r)|^2\sin(qr)dr \; . \tag{B3}$$

$\epsilon_{\mathrm{Si}}(q)$ is the q-dependent dielectric function taken from Ref. 30, $\varphi_s(r)$ is the radial part of the wave function φ_s, which is obtained from the atomic-structure calculations of Ref. 29. A similar technique is applied to the case of U_{sp} and U_{pp}. We obtain

$$U_{ss}=3.84 \text{ eV}, \quad U_{sp}=3.05 \text{ eV}, \quad U_{pp}=2.54 \text{ eV} \; . \tag{B4}$$

These values are only about three times smaller than in the free atom, i.e., for $\epsilon_{\mathrm{Si}}=1$. This is due to the fact that the screening is not so efficient because of the short distance between the two electrons on the same atom. Note, however, that Coulomb energies are the main contributions in the exchange integrals of the excitonic calculation. Finally, we have also evaluated the intra-atomic exchange integrals. They are, for example,

$$\int \frac{\varphi_s^*(1)\varphi_{p_x}^*(2)\varphi_s(2)\varphi_{p_x}(1)}{\epsilon_{\mathrm{Si}}r_{12}}d^3r_1\,d^3r_2 \; ,$$
$$\int \frac{\varphi_{p_y}^*(1)\varphi_{p_x}^*(2)\varphi_{p_y}(2)\varphi_{p_s}(1)}{\epsilon_{\mathrm{Si}}r_{12}}d^3r_1\,d^3r_2 \; . \tag{B5}$$

All the other integrals can be deduced from these by symmetry. For the free atoms, they can be obtained following the rules discussed by Slater.[31] It is usually found that intra-atomic exchange integrals are ten times smaller than intra-atomic Coulomb integrals.[31] Here the problem is much more complex because of the dielectric function in the integral. Therefore, using the same scaling rule, we have fixed all the integrals in Eq. (B5) at 0.3 eV. We have verified that our results do not depend on the exact numerical value of these terms.

The calculated exchange splitting is dependent on the direction of the asymmetric crystallite. For an ellipsoid in the X direction, the highest valence state is mainly p_X-like. Therefore, for a (100) direction, the confined state is mainly built from the p_x Bloch states. In the conduction band, for a (100) direction, there exist two kinds of confinement. States arising from the (100) and (-100) valleys are higher in energy than states arising from (010), (0-10), (001), and (00-1) valleys because of the anisotropy of the effective masses in the conduction band. The same is obtained for the confinement in wires.[17] The states arising from (010), (0-10), (001), and (00-1) valleys mainly behave like p_y and p_z. In consequence the exchange integrals are, for example, of the form $\langle \psi_{p_x}^v(1)\psi_{p_y}^c(2)|(e^2/\epsilon_{\mathrm{Si}}r_{12})|\psi_{p_y}^c(1)\psi_{p_x}^v(2)\rangle$ where $\psi_{p_x}^v$ and $\psi_{p_y}^c$ are, respectively, the p_x-like valence and p_y-like conduction states. When we develop this integral in the atomic-orbital basis, the main contributions come from the intra-atomic exchange integrals like $\langle \varphi_{p_x}(1)\varphi_{p_y}(2)|(e^2/\epsilon_{\mathrm{Si}}r_{12})|\varphi_{p_y}(1)\varphi_{p_x}(2)\rangle$, which are small. In contrast, for a crystallite in the (111) direction, both the valence and conduction states are built from p_x-like, p_y-like, and p_z-like Bloch states together. Development of the exchange integral in the atomic basis gives, in addition to the previous case, intra-atomic Coulomb integrals like $\langle \varphi_{p_x}(1)\varphi_{p_x}(2)|(e^2/\epsilon_{\mathrm{Si}}r_{12})|\varphi_{p_x}(1)\varphi_{p_x}(2)\rangle$, which are much more important than the intra-atomic exchange integrals.

APPENDIX C: STOKES SHIFT DUE TO THE LATTICE RELAXATION

Here we give details on the simple elastic model used to calculate the atomic relaxation induced by an exciton in spherical-silicon nanocrystallites. Let us consider that for a spherical crystallite of radius R one creates an electron-hole pair. In the effective-mass approximation, the electron-hole density is given by

$$n(r)=\frac{1}{2\pi R}\left[\frac{\sin(\pi r/R)}{r}\right]^2 , \tag{C1}$$

where r is the distance from the center of the crystallite. As the deformations depend on the electron-hole density, we can assume in first approximation that the displacement $\mathbf{u}(x,y,z)$ of point $M(x,y,z)$ of the crystallite is radial, i.e., $\mathbf{u}=u(r)\mathbf{e}_r$. As the density $n(r)$ is a slowly variable function of the position r, we can write the energy density at r, to first order

$$E(r)=E_0(r)+E_g(r)n(r) \; , \tag{C2}$$

where $E_0(r)$ is the ground-state energy density and $E_g(r)$ is the excitonic band-gap energy. Both are taken to depend upon r if we assume that there can exist a local deformation induced by the existence of $n(r)$. The deformations are characterized classically by the strain parameters[32]

$$e_{ij}=\frac{1}{2}\left[\frac{\partial u_i}{\partial x_j}+\frac{\partial u_j}{\partial x_i}\right] . \tag{C3}$$

The variation of energy density with respect to the ground state (before electron excitation) is the sum of the elastic energy density and of the electron-hole energy density[32]

$$\Delta E(r)=\frac{C_{11}}{2}(e_{xx}^2+e_{yy}^2+e_{zz}^2)+\frac{C_{44}}{2}(e_{yz}^2+e_{zx}^2+e_{xy}^2) + C_{12}(e_{yy}e_{zz}+e_{zz}e_{xx}+e_{xx}e_{yy})+E_g(r)n(r) \; , \tag{C4}$$

where C_{11}, C_{12}, and C_{44} are taken as the elastic constants of the bulk silicon because the bonds between silicon atoms are not much influenced by the confinement. With radial displacements $u(r)\mathbf{e}_r$, the strain parameters at $M(x,y,z)$ are given by

$$e_{ii}=\left[\frac{x_i}{r}\right]^2\left[\frac{\partial u}{\partial r}\right]+\frac{u}{r}\left[\frac{r^2-x_i^2}{r^2}\right],$$
$$e_{ij}=\frac{x_i x_j}{r^2}\left[\left[\frac{\partial u}{\partial r}\right]-\frac{u}{r}\right],\quad i\neq j, \tag{C5}$$

where the x_i are equal to either x, y, or z and $u=u(r)$. The excitonic band-gap energy $E_g(r)$ is also dependent on the deformations. We have supposed that it follows the variations of the band extrema in bulk silicon in the same conditions of strains, i.e., $E_g(r)=E_c(r)-E_v(r)$. For the conduction band, $E_c(r)$ is taken as the minimum of the six valleys, which are no longer equivalent under the action of the strains. Their variations with the strains are defined by the deformation potentials Ξ_d and Ξ_u.[33] Their minimum $E_c(r)$ is given by[33]

$$E_c^0+\Xi_d(e_{xx}+e_{yy}+e_{zz})+\min(\Xi_u e_{xx},\Xi_u e_{yy},\Xi_u e_{zz}), \tag{C6}$$

where E_c^0 is the conduction-band minimum without strain. For the behavior of the valence band under strains, we use the derivation of Pikus and Bir where the energies are obtained by the diagonalization of a 6×6 matrix.[34] Matrix elements depend on the strain parameters and on the deformation potentials a_v, b_v, and d_v. a_v is the valence-band hydrostatic deformation potential, b_v is the valence-band shear deformation potential associated with strain along the (100) crystallographic direction, and d_v is the shear deformation potential for strain along the (111) direction. $E_v(r)$ is taken as the maximum energy obtained after diagonalization.

It must be noted that the conduction-band minimum of Eq. (C6) and the valence-band maximum obtained by diagonalization of the 6×6 matrix[34] have not the full spherical symmetry but the tetrahedral T_d symmetry. As a consequence, $E_c(r)$ and $E_v(r)$ do not depend only on the distance from the origin r as assumed in the notation. To take into account the full dependence of the energies in the calculation leads to severe and unnecessary computational difficulties. In particular, this shows that strictly speaking the displacements are not fully radial. However, we believe that to assume a spherical symmetry cannot lead to a large error, in particular because of the spherical symmetry of the electron-hole density. For the conduction band, we have defined $E_c(r)$ as the average of Eq. (C6) over the directions, which can be done quite easily—nearly analytically—in regard to the simple expression in Eq. (C6). In contrast, this is much more difficult to do for the valence band. Therefore, $E_v(r)$ has been defined as its value in the (100) direction, i.e., at a point $M(r,0,0)$. We have verified that taking another direction does not change significantly the final results.

The variation in total energy of the system after excitation of an electron is made by integration of the energy density of Eq. (C4) over the volume of the crystallite. This is easily done since all the terms have now the spherical symmetry. Then the total energy is minimized with respect to the displacement $u(r)$. In practice, $u(r)$ is written as a Fourier sum whose coefficients are adjusted to get the minimum of the energy functional. The minimization is performed using a conjugate-gradient method.

Results are plotted in Fig. 9. The continuous line corresponds to the case where the deformation potentials injected in the calculation are those of the bulk silicon crystal.[35] The other curves are obtained by changing substantially Ξ_d or Ξ_u (or both) to check the sensitivity of the results on these parameters (we recall that they actually depend on the confinement). Anyway, Fig. 9 shows that the Franck-Condon shift must be substantial, in the meV range.

[1]B. K. Meyer, D. M. Hofmann, W. Stadler, V. Petrova-Koch, F. Koch, P. Omling, and P. Emanuelsson, Appl. Phys. Lett. **63**, 2120 (1993).

[2]J. P. Proot, C. Delerue, and G. Allan, Appl. Phys. Lett. **61**, 1948 (1992); C. Delerue, G. Allan, and M. Lannoo, in *Optical Properties of Low Dimensional Silicon Structures,* Vol. 244 of *NATO Advanced Study Institute, Series E,* edited by D. C. Bensahel, L. T. Canham, and S. Ossicini (Kluwer, Dordrecht, 1993), p. 229; Phys. Rev. B **48**, 11 024 (1993).

[3]A. Bsiesy, J. C. Vial, F. Gaspard, R. Hérino, M. Ligeon, F. Muller, R. Romestain, A. Wasiela, A. Maimaoui, and G. Bomchil, Surf. Sci. **254**, 195 (1991).

[4]P. D. J. Calcott, K. J. Nash, L. T. Canham, M. J. Kane, and D. Brumhead, J. Phys. Condens. Matter **5**, L91 (1993).

[5]I. Sagnes, A. Halimaoui, G. Vincent, and P. A. Badoz, Appl. Phys. Lett. **62**, 1155 (1993).

[6]P. D. J. Calcott, K. J. Nash, L. T. Canham, M. J. Kane, and D. Brumhead, in *Microcrystalline Semiconductors—Materials Science & Devices,* edited by P. M. Fauchet, C. C. Tsai, L. T. Canham, I. Shimizu, and Y. Aoyagi, MRS Symposia Proceedings No. 283 (Materials Research Society, Pittsburgh, 1993), p. 143.

[7]X. L. Zheng, W. Wang, and H. C. Chen, Appl. Phys. Lett. **60**, 986 (1992).

[8]J. C. Vial, A. Bsiesy, G. Fishman, F. Gaspard, R. Hérino, M. Ligeon, F. Muller, R. Romestain, and R. M. Macfarlane, in *Microcrystalline Semiconductors—Material Science & Devices* (Ref. 6), p. 241.

[9]J.-C. Merle, M. Capizzi, P. Fiorini, and A. Frova, Phys. Rev. B **17**, 4821 (1978).

[10]G. Fishman, R. Romestain, and J. C. Vial, J. Phys. IV **3**, 355 (1993).

[11]C. Tserbak, H. M. Polatoglou, and G. Theodorou, Phys. Rev. B **47**, 7104 (1993).

[12]Y. Kayanuma, Solid State Commun. **59**, 405 (1986).

[13]D. Babic, R. Tsu, and R. F. Greene, Phys. Rev. B **45**, 14 150 (1992).

[14]J. C. Vial, A. Bsiesy, F. Gaspard, R. Hérino, M. Ligeon, F. Muller, R. Romestain, and R. M. Macfarlane, Phys. Rev. B **45**, 14 171 (1992).

[15]M. S. Hybertsen and M. Needels, Phys. Rev. B **48**, 4608 (1993).

[16]W. L. Wilson, P. F. Szajowski, and L. E. Brus, Science **262**, 1242 (1993); K. A. Littau, P. J. Szajowski, A. J. Muller, A. R. Kortan, and L. E. Brus, J. Phys. Chem. **97**, 1224 (1993).

[17]M. Voos, Ph. Uzan, C. Delalande, G. Bastard, and A. Halimaoui, Appl. Phys. Lett. **61**, 1213 (1992).

[18]R. Tsu and D. Babic, in *Optical Properties of Low Dimensional Silicon Structures,* Vol. 244 of *NATO Advanced Study Institute, Series E,* edited by D. C. Bensahel, L. T. Canham, and S. Ossicini (Kluwer, Dordrecht, 1993), p. 203.

[19]M. S. Hybertsen, Phys. Rev. Lett. **72**, 1514 (1994); Y. H. Xie, M. S. Hybertsen, W. L. Wilson, S. A. Ipri, G. E. Carver, W. L. Brown, E. Dons, B. E. Weir, A. R. Kortan, G. P. Watson, and A. J. Liddle, Phys. Rev. B **50**, 8138 (1994).

[20]D. Bellet, G. Dolino, M. Ligeon, P. Blanc, and M. Krisch, J. Appl. Phys. **71**, 145 (1992).

[21]J. Bourgoin and M. Lannoo, in *Point Defects in Semiconductors II,* edited by M. Cardona (Springer, Berlin, 1981).

[22]*Properties of Silicon,* EMIS Data Reviews Series No. 4 (INSPEC, The Institution of Electrical Engineers, New York, 1988).

[23]K. J. Chang, S. Froyen, and M. L. Cohen, Solid State Commun. **50**, 105 (1984).

[24]N. Ookubo, Y. Matsuda, and N. Kuroda, Appl. Phys. Lett. **63**, 346 (1993).

[25]J. Camassel, E. Massone, L. Lyapin, J. Allegre, P. Vincente, A. Foucaran, A. Raymond, and J. L. Robert, in *Proceedings of the International Conference on Physics of Semiconductors,* edited by P. Jiang and H.-Z. Zheng (World Scientific, Singapore, 1992), p. 1463.

[26]W. Zhou, M. Dutta, H. Shen, J. F. Harvey, R. A. Lux, C. H. Perry, R. Tsu, N. M. Kalkhoran, and F. Namovar, Appl. Phys. Lett. **61**, 1435 (1992).

[27]J. M. Ryan, P. R. Wansley, and K. L. Bray, Appl. Phys. Lett. **63**, 2260 (1993).

[28]R. S. Knox, in *Solid State Physics, Supplement 5,* edited by F. Seitz and D. Turnbull (Academic, City, 1963).

[29]F. Herman and S. Skillman, *Atomic Structure Calculations* (Prentice-Hall, New York, 1963).

[30]G. Cappelini, R. Del Sole, L. Reining, and F. Bechstedt, Phys. Rev. B **47**, 9892 (1993).

[31]J. C. Slater, *Quantum Theory of Atomic Structure* (McGraw-Hill, City, 1960), Vols. 1 and 2.

[32]C. Kittel, *Introduction to Solid State Physics* (Wiley, New York, 1971).

[33]L. D. Laude, F. H. Polak, and M. Cardona, Phys. Rev. B **3**, 2623 (1971).

[34]G. E. Pikus and G. L. Bir, Fiz. Tverd. Tela (Leningrad) **1**, 1642 (1959) [Sov. Phys. Solid State **1**, 1502 (1960)].

[35]D. D. Nolte, W. Walukiewick, and E. E. Haller, Phys. Rev. B **36**, 9392 (1987).